LIMITATIONS IN GPS POSITIONING ACCURACIES AND RECEIVER TRACKING PERFORMANCE DURING SOLAR MAXIMUM

S. Skone, M. El-Gizawy and S.M. Shrestha
Department of Geomatics Engineering
University of Calgary
2500 University Dr. NW
Calgary, Alberta, Canada T2N 1N4
Email contact: sskone@geomatics.ucalgary.ca

BIOGRAPHY

Susan Skone is an Assistant Professor in the Department of Geomatics Engineering, University of Calgary. She has B.Sc. degrees in math and physics (1989,1990), and an M.Sc. in space physics (1994), fom the University of Alberta. She also has a Ph.D. in Geomatics Engineering (1998) from the University of Calgary. Her research focuses on ionosphere modelling for GPS applications.

Mahmoud L. El-Gizawy is an M.Sc. student in the Department of Geomatics Engineering, University of Calgary. He obtained his B.Sc. in 1999 from Ain Shams University, Cairo, Egypt.

Sudhir Shrestha completed an M. Sc. in Surveying Engineering from Moscow State University of Geodesy and Cartography in 1994. He has worked in the Survey Department of Nepal (1994-1999) as a survey engineer monitoring plate movement using GPS. He has also completed a Professional Masters course on GIS from ITC Netherlands. Sudhir has been an M. Sc. student in the Department of Geomatics Engineering, University of Calgary since September 2000.

ABSTRACT

GPS signals are refracted by the dispersive ionosphere, resulting in ranging errors dependent on both the given signal frequency and ionospheric total electron content (TEC). Such range errors translate into a degradation of positioning accuracy. While it is possible to mitigate the impact of ionospheric effects on GPS positioning applications, through differential techniques (DGPS) and/or ionosphere modelling, residual errors may persist in regions where steep gradients or localised irregularities in electron density exist – particularly during periods of high geomagnetic activity. In addition, loss of GPS signal availability can occur in regions where small-scale irregularities in electron density cause amplitude fading and phase scintillations. Such effects are increased with enhanced ionospheric activity and are an issue for the reliable implementation of safety-critical GPS systems.

A solar maximum was observed mid-late 2000, with associated degradations in GPS positioning accuracies and receiver tracking performance, while geomagnetic storm activity is expected to expected to peak in the following years (2001-2003). In this paper, the impact of solar maximum and storm activity on GPS applications is investigated, with a focus on the high latitude auroral region and the low latitude anomaly region. Long-term trends are studied using data from permanent GPS reference networks in Canada, the United States and Brazil. Degradations in GPS performance are quantified in terms of receiver tracking performance and enhanced differential and single point positioning errors.

1. INTRODUCTION

The ionosphere is a dispersive medium, in which RF signals are refracted by an amount dependent on the given signal frequency and the electron density, resulting in a range error:

$$I = \pm 40.3 \frac{TEC}{f^2} \qquad \text{(in metres)} \qquad (1)$$

where TEC denotes the total electron content integrated along a 1 m^2 column along the signal path (in el/m^2), f is the signal frequency (in Hz), and + (-) denotes the group delay (phase advance). The dispersive nature of the ionosphere allows direct calculation of the absolute TEC, if range measurements are available on two separate frequencies:

$$TEC = \frac{1}{40.3}\left(\frac{1}{f_1^2} - \frac{1}{f_2^2}\right)^{-1}(P_1 - P_2 - b_r - b_s) \qquad (2)$$

for the case of a dual-frequency GPS receiver, where f_1 = 1575.42 MHz (herein referred to as L1) and f_2 = 1227.60 MHz (herein referred to as L2), P denotes the pseudorange observable, and b_r and b_s are receiver and satellite interchannel bias terms, respectively. For convenience, the TEC is usually expressed in units of TECU (10^{16} el/m^2), where 1 TECU translates to 0.16 m for the L1 observable. TEC estimates derived using Equation 2 are corrupted by noise and multipath effects, which are typically on the order of 1-5 TECU RMS. More precise estimates of the TEC can be obtained as follows:

$$\mathrm{TEC} = \frac{-1}{40.3}\left(\frac{1}{f_1^2}-\frac{1}{f_2^2}\right)^{-1}\left(\Phi_1 - \Phi_2 - \lambda_1 N_1 + \lambda_2 N_2 - b_r' - b_s'\right) \quad (3)$$

where Φ represents the ambiguous carrier phase range and N represents the carrier phase ambiguity (in cycles). The ambiguities must be known in order to calculate absolute TEC using Equation 3. Ambiguous phase ranges are useful, however, in deriving information about relative variations in TEC, provided that the ambiguities and biases remain constant over time:

$$\mathrm{TEC} = \frac{-1}{40.3}\left(\frac{1}{f_1^2}-\frac{1}{f_2^2}\right)^{-1}\left(\Phi_1 - \Phi_2\right) \quad (4)$$

Such TEC estimates have a relative accuracy of better than 0.10 TECU RMS, and can be used to analyse relative spatial and temporal variations in TEC. The magnitude of TEC depends on slant path through the ionosphere, such that slant TEC values are 3 times larger at elevation angles of 5 degrees, versus vertical TEC (at 90 degrees elevation).

Larger magnitudes of TEC can lead to enhanced single point positioning errors for single frequency users, while the presence of large-scale gradients and smaller-scale features in TEC can result in a degradation of differential positioning accuracies and limitations in ambiguity resolution. In addition, irregularities in electron density can cause scintillation of the RF signals and degraded receiver tracking performance, particularly for the L2 signal. Such ionospheric effects are a function of latitude, season, storm activity and solar cycle. Brief descriptions of various ionospheric effects and phenomena are given in the next section.

2. IONOSPHERIC PHENOMENA

A variety of ionospheric phenomena take place in different regions of the Earth's ionosphere. Long-term trends may be observed at all latitudes, while localised features such as the equatorial anomaly are present only in limited regions. Short-term variations in ionospheric electron density are observed at high latitudes during transient substorm events. Prior to analysing the impact of such effects on GPS positioning applications, it is useful to provide an overview of global and local phenomena in the Earth's ionosphere.

2.1 Variability of TEC

It has been well established that diurnal variations of TEC are controlled by solar radiation, with a dayside maximum at 1400 local time. Dayside values are generally a factor of 2-4 larger than the nightside TEC. The magnitude of TEC can also vary significantly with sunspot number (solar cycle) and season. *Klobuchar et al.* [1995] observed an enhancement of TEC by a factor of 2-3 for solar maximum, versus solar minimum, conditions at the mid-latitudes. *Soicher and Gorman* [1985] also observed seasonal variations at mid-latitudes, with TEC values being larger in the winter, versus summer, months. The basic cause of this winter anomaly is thought to be the transport of air masses into the mid-latitude mesosphere and lower thermosphere from other regions – leading to an enhancement of observed TEC. Such seasonal variations also take place at the higher latitudes, and annual peaks in equatorial TEC are observed during the equinoctial months. Formation of the equatorial anomaly is discussed in Section 2.5.

2.2 Auroral Region

The auroral oval (Figure 1) is a high latitude region of the Earth's ionosphere, where dynamic ionospheric phenomena take place. The unique nature of this region derives from complex interactions between the terrestrial magnetic field and charged particles flowing outwards from the Sun (solar wind). During periods of enhanced solar-terrestrial interaction, electrons are accelerated from near-Earth regions, along the terrestrial magnetic field lines, into the high latitude ionosphere. These electrons are energized through interactions between the solar wind and the Earth's magnetic field, resulting in optical and UV emissions commonly known as the aurora borealis/australis. This phenomenon characterizes the geomagnetic or magnetospheric substorm.

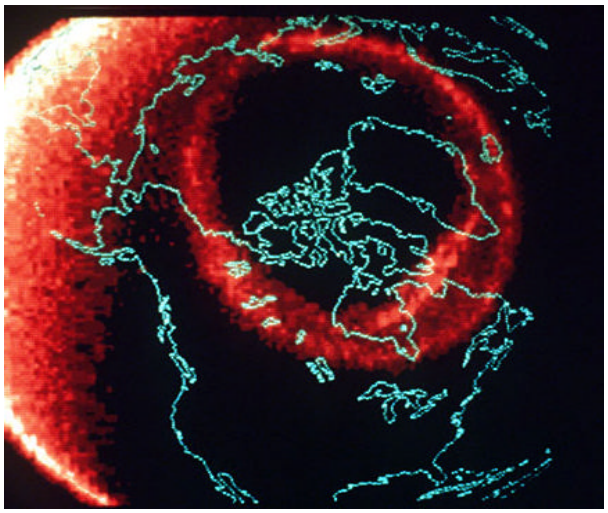

Figure 1. Satellite image of the auroral oval.

Auroral intensifications, during a substorm event, have times scales on the order of 15 minutes and, for intense events, multiple intensifications can take place over a period of hours. The auroral oval can expand several degrees equatorward during such events (i.e. over the Northern United States and Europe). Irregular precipitation of electrons during substorms, and the presence of localised electric currents, can result in structured depletions/enhancements of TEC in the auroral ionosphere (at E-region altitudes of 110 km). *Hunsucker et al.* [1995] determined that these features are medium-scale structures (20-130 km in wavelength) with amplitudes of 1-5 TECU (16 – 80 cm ionospheric range delay on L1). Such structures can be difficult to model and can result in a degradation of precise positioning applications where ambiguities cannot be resolved.

Ionization along terrestrial magnetic field lines also results in small-scale field-aligned irregularities in electron density at F region (350 km) altitudes. These irregularities have scale sizes on the order of 1 km or less, and can cause phase and amplitude scintillations – with associated degradations in GPS receiver tracking performance. During periods of scintillation, rapid random phase variations can cause the GPS receiver to lose phase lock. Amplitude fades (loss of signal strength) can also persist, resulting in the loss of GPS tracking and navigation capabilities. Scintillations are often observed in conjunction with the medium-scale TEC structures during auroral substorm events [*Basu et al*., 1983].

2.3 Sub-Auroral Region

Enhanced electric fields are also present near the equatorward auroral boundary during geomagnetically disturbed periods, which can lead to a depletion of electron density at sub-auroral latitudes. The resulting gradients in TEC can cause differential ionospheric range errors in and near the auroral region, leading to degradation of DGPS positioning accuracies. Such large-scale gradients exist at an ionospheric trough below the equatorward boundary of the auroral oval, at sub-auroral latitudes of 45° - 55° geographic in the North American sector. This feature is present in both the nightside and dayside local time sectors, with the largest gradients observed post-noon into dusk. Gradients in this region can persist for several hours, with differential ionospheric range residuals of 15 ppm [*Foster*, 2000]. Regions of dayside storm-enhanced electron density (SED) can also occur during more global magnetic storm events, with ionosphere gradients as large as 70 ppm at latitudes of 50° geographic [*Foster*, 2000]. This effect can also persist for several hours.

2.4 High Latitude Ionospheric Activity Indices

Ionospheric activity at the auroral and sub-auroral latitudes is often described as a function of geomagnetic variations. During periods of enhanced auroral activity the magnitude of strong electric currents is reflected in magnetic field variations at the Earth's surface. Such currents tend to fluctuate in response to transient storm events. A geomagnetic index therefore provides an approximate measure of ionospheric activity.

Geomagnetic indices are derived using measured variations in magnetic field strength at globally distributed sub-auroral (and auroral) ground-based magnetometer stations. The Kp three-hourly global index [*Mayaud*, 1980] is often used to describe levels of global ionospheric activity. Local three-hourly K indices can also be derived for a given magnetometer station, such that the level of local activity may be quantified in a given region. K indices range from 0 to 9, with 9 representing the highest level of ionospheric activity.

Figure 2 shows three-hourly local K indices for the North American sector during 1997-2001, where K values of 5-6 indicate a moderate storm event and K values greater than 6 reflect major-intense storm activity. Moderate storm events have occurred relatively frequently since 1997, while only 15 periods with K values greater than 6 have been observed during this solar cycle. Note that significant storm activity occurred during 1998, several years before solar maximum. The frequency and

magnitude of geomagnetic storm events tends to peak several years before and after solar maximum; storm events are expected to occur once every few months during 2002-2003 [*Kunches*, 1997].

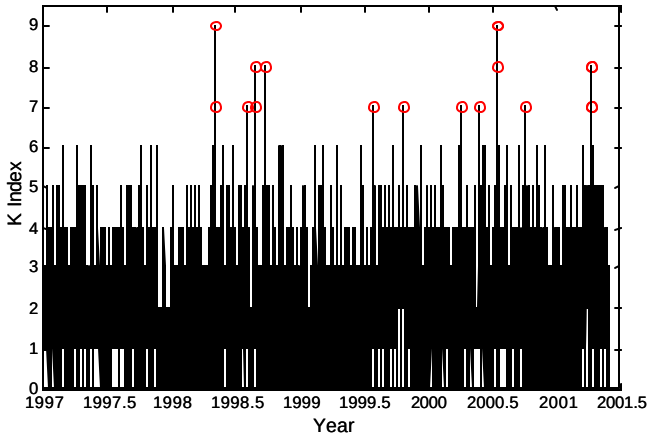

Figure 2. Local K indices for Fredericksburg Virginia (38.2° N, 77.4° W) during 1997-1998 and Boulder Colorado (40.0° N, 105.3° W) during 1999-2001. K indices greater than 6 (red circles) represent major-intense storm activity.

2.5 Equatorial Anomaly

The largest global TEC values are generally observed in the equatorial region, as a result of stronger incident solar radiation and, therefore, enhanced ionization. A feature of the equatorial ionosphere is the equatorial, or Appleton, anomaly [*Appleton*, 1954]. This anomaly consists of two maxima in electron density, located approximately 10-15° north and south of the magnetic equator (Figure 3). This feature is controlled by an E-region dynamo that is driven by global tidal winds, resulting in a zonal electric field at the magnetic equator. In the dayside to postsunset local time sector, this electric field is directed west-to-east, creating an **E**×**B** drift velocity that is directed upwards and away from the magnetic equator (the "fountain effect"). This allows electrodynamic lifting of the equatorial plasma to F region heights of 800 km and beyond, and enhanced electron densities exist in the region ±20° magnetic latitude. In the post-midnight sector, the equatorial electric field is generally directed westward, resulting in the opposite effect – a lowering of ionospheric plasma towards the magnetic equator.

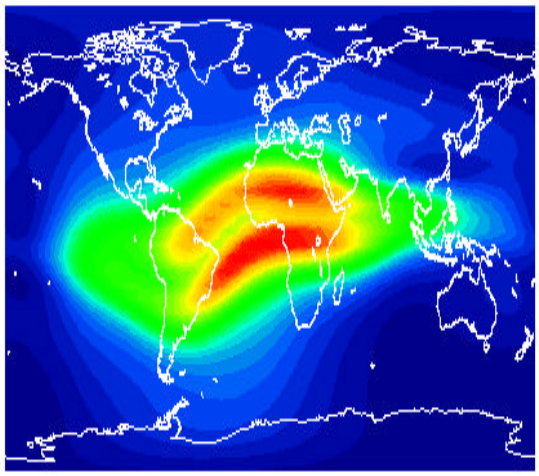

Figure 3. Global distribution of total electron at 1400 UT. The double-peaked equatorial anomaly is observed on the dayside, aligned parallel to the magnetic equator.

The daily equatorial anomaly generally begins to develop around 0900-1000 local time, reaching its maximum development at 1400-1500 [cf. *Huang and Cheng*, 1991]. In periods of solar maximum, however, the anomaly may peak at ≈2100 local time, and gradients in TEC are considerably larger at this secondary diurnal maximum. During the previous solar maximum, *Wanninger* [1993] observed north-south TEC gradients as large as 30 TECU per 100 km (48 ppm for L1 ionosphere range delay) in the postsunset anomaly region. Seasonal peaks in equatorial TEC are observed during the equinoctial months.

Irregularities in electron density can also develop in the postsunset anomaly. As plasma is lifted to higher altitudes, "bubbles" (plasma depletions) rise into the ionosphere in patches aligned with the Earth's magnetic field, up to heights of 1000 km [cf. *Aarons et al*., 1983]. Small-scale irregularities develop in steep gradients along the walls of these bubbles - a source of intense scintillation effects. This effect has been observed to peak at approximately 2100 local time, with maximum intensity near the anomaly peaks (±10° magnetic) [*Basu et al*., 1988]. Seasonal variations in scintillations have been observed, with peaks during the months October-November and February-March (South American sector). Scintillation effects are generally largest during periods of solar maximum.

3. TEC VARIATIONS – SOLAR CYCLE 23

The current solar cycle reached a peak in mid-2000, as illustrated in observed variations of the sunspot number pictured in Figure 4. In order to analyse the various trends in TEC during the period of solar maximum, dual frequency data from the period 1998-2001 were processed for three stations of the International GPS Service (IGS) network: Churchill (CHUR), United States Naval Observatory (USNO) and Arequipa (AREQ). CHUR, USNO and AREQ were chosen to be representative of the high, middle, and low latitudes, respectively, in the North and South American sectors. Locations of the three stations are shown in Figure 5. Observation and broadcast ephemeris files were available in RINEX format for each station, with an observation sample interval of 30 s.

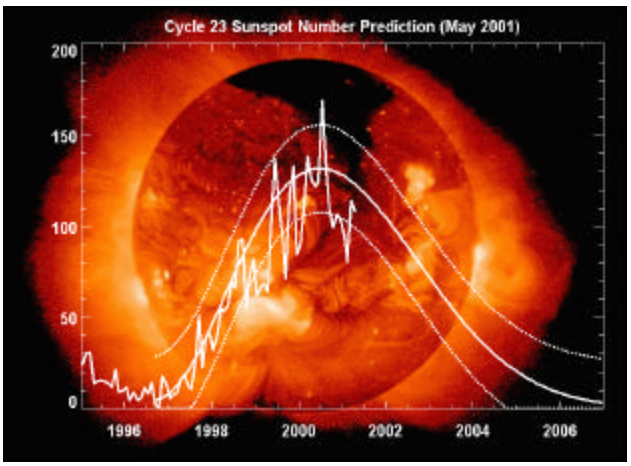

Figure 4. Sunspot numbers for solar cycle 23 (courtesy of NASA).

Dual frequency observations from each station were processed independently using a single station vertical TEC estimation algorithm. This algorithm is based on a Kalman filter approach, where precise relative TEC estimates (Equation 4) are used to smooth the TEC values derived from pseudoranges (Equation 2). The TEC is modelled as a polynomial expansion (in geomagnetic latitude and local time) in the vicinity of the reference station, where parameters describing the vertical TEC and interchannel biases are estimated simultaneously with accuracies of 1-2 TECU. The ionosphere modelling software, TECANALYS™, was developed at the University of Calgary.

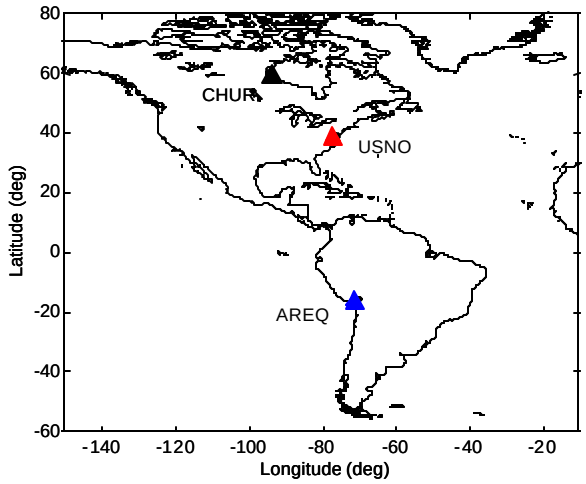

Figure 5. Reference stations Churchill (CHUR), United States Naval Observatory (USNO) and Arequipa (AREQ) in the IGS network.

Vertical TEC values at 1400 local time are plotted for each day of the years 1998-2001 in Figure 6, for each of the three stations. These values are representative of the maximum diurnal values. Note that several gaps exist in the plot for station AREQ – these are periods when no data were available. Several trends are observed in this figure:

1) A general enhancement of TEC values with solar cycle is observed for all three stations, with TEC estimates being larger at all latitudes for year 2000 versus 1998.

2) TEC values are consistently larger by a factor of approximately 2 for the low latitude station (AREQ) versus the middle (USNO) and high (CHUR) latitude stations.

3) Seasonal variations in TEC are observed for all three stations, with the largest TEC values during the winter months – primarily in October-November and February-March. Such trends arise from the winter anomaly at high and mid-latitudes, and enhancement of the equatorial anomaly at low latitudes during the equinoxes. These seasonal variations are enhanced at solar maximum (year 2000).

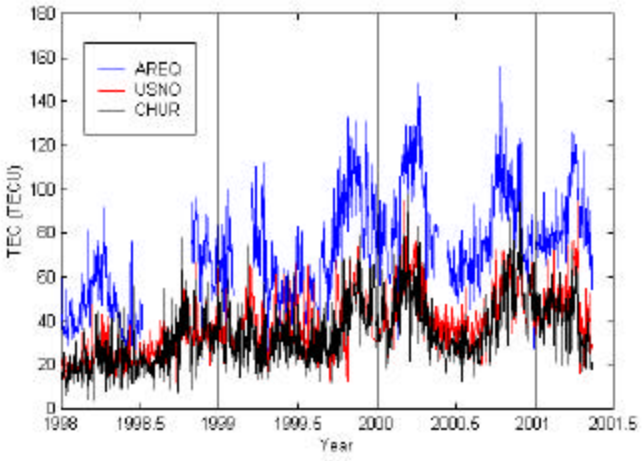

Figure 6. Vertical TEC estimates at 1400 local time for the high (CHUR), middle (USNO) and low (AREQ) latitude stations.

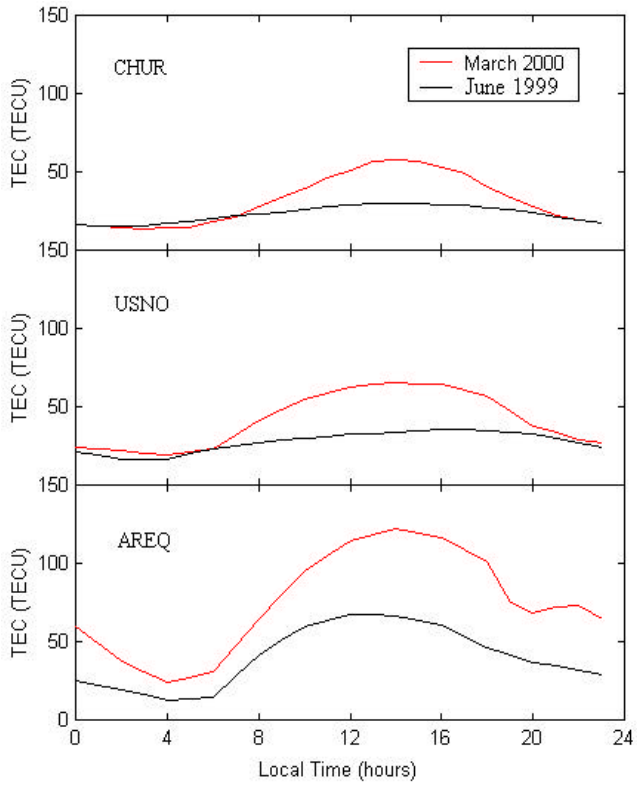

Figure 7. Comparison of diurnal vertical TEC variations for March 2000 and June 1999, for the high (CHUR), middle (USNO) and low (AREQ) latitude stations. Vertical TEC values represent monthly means for each hour of local time.

Figure 7 shows a comparison of diurnal variations in TEC for summer (June 1999) versus the equinox (March 2000) at each of the three reference stations. These plots are derived by computing mean TEC estimates for each hour of local time, at each station, based on the full month of observations. In general, TEC values are a factor of 2 larger for March versus June. Daily peak values of TEC are consistently observed at approximately 1400 local time for all stations. At the lower latitudes, however, an enhancement of the secondary diurnal peak is observed at approximately 2200 local time during March 2000. This is a feature unique to the lower latitudes, where the secondary peak arises from equatorial electric fields and the associated fountain effect (see Section 2.5). Very large gradients in TEC and scintillation effects can be present near this secondary peak.

4. SINGLE POINT POSITIONING ACCURACIES

The recent removal of Selective Availability in May 2000 should allow single point positioning accuracies of 22 m horizontal and 33 m vertical at the 95% level for single frequency users [*Shaw et al.*, 2000]. The quoted accuracies are based on GPS signal specifications for the Standard Positioning Service (SPS), which includes an assumed ionospheric range error of 7 m. Based on the TEC values observed in Figure 6, however, and the direct dependence of GPS range errors on TEC (Equation 1), it is inferred that positioning errors may vary widely with location and season.

Vertical single point position estimates are biased by the ionospheric range errors. In the horizontal plane, correlated ionospheric range errors are compensated to a large extent through the horizontal geometry of the range observations. In order to investigate the impact of ionospheric effects on single point positioning accuracies, position solutions were computed for each of the three stations in Figure 5. Troposphere corrections were applied to the observations and position estimates were computed using the L1 code observations for an elevation cutoff angle of 10 degrees. Comparisons were made with known station coordinates and 95th-percentile statistics were computed every 30 minutes, based on 30 s position estimates. Only those estimates with HDOP (VDOP) less than 2 were included in statistics for the horizontal (vertical) position estimates. While results presented here are derived for survey-grade receivers, it is assumed that such results are representative of positioning accuracies which may be achieved using lower-cost single frequency receivers.

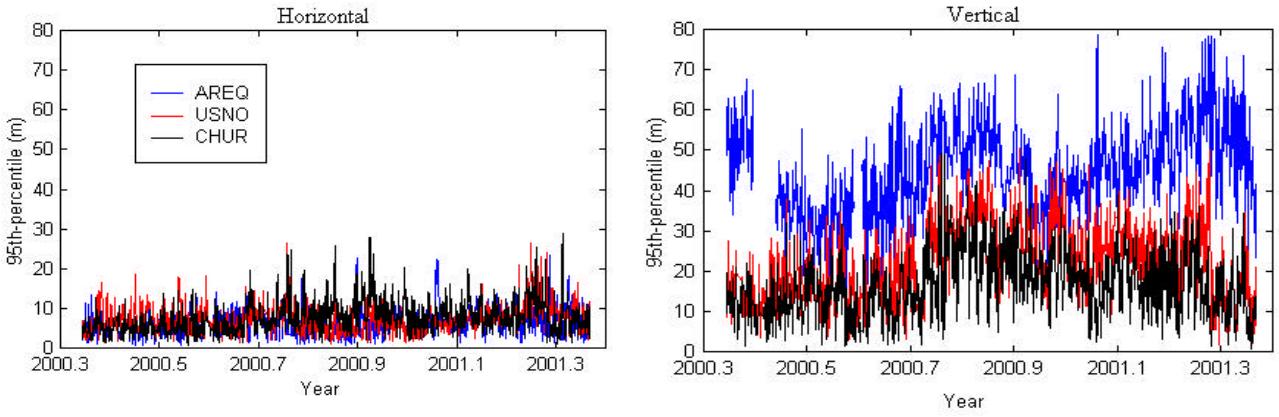

Figure 8. 95th-percentile horizontal and vertical positioning accuracies for the high (CHUR), middle (USNO) and low (AREQ) latitude stations.

Figure 8 shows horizontal and vertical positioning accuracies for the three stations, for the post-SA period May 2000 – May 2001. Only values for the local time sector 1330 to 1430 are plotted, in order to show the maximum diurnal values. Horizontal errors are generally less than 20 m (95th-percentile) for all three stations, indicating minimal dependence on the magnitude of ionospheric TEC values, as expected. For the vertical position errors, however, a clear dependence on the TEC values is observed, with significantly larger position errors at the lower latitudes. Seasonal variations are evident, with larger vertical positioning errors in October and March for all three stations during the period of solar maximum. Depending on location and season, dayside position errors may vary between between 2 and 60 m at the 95% confidence level.

5. DIFFERENTIAL POSITIONING ACCURACIES

In order to mitigate the impact of ionospheric errors on positioning accuracies, single difference and double difference techniques are often employed to reduce the ionospheric range errors and, for shorter baseline applications, resolve carrier phase ambiguities. Typically, large-scale gradients in TEC can result in differential ionosphere range delays on the order of 1-2 ppm [*Parkinson and Enge*, 1996]. As stated in Section 2, however, TEC gradients can be significantly larger in both the high latitude auroral and sub-auroral regions, and in the low latitude equatorial anomaly region – resulting in a degradation of DGPS positioning accuracies. This section focuses on limitations in differential positioning accuracies in the near-equatorial low latitude, sub-auroral and auroral regions, where some of the largest TEC gradients in the Earth's ionosphere may be observed.

5.1 Low Latitudes

5.1.1 TEC Gradients

Larger TEC values are observed during the equinoctial months at all latitudes (Figure 6). For the lower latitudes, the larger TEC values reflect an enhancement of the equatorial anomaly, with a main peak at 1400 local time and a secondary peak at 2100 local time. This secondary peak is enhanced particularly during the period of solar maximum and associated gradients can be very large in the north-south direction.

In order to investigate the magnitude of TEC gradients at low latitudes, data from reference stations in the Brazilian RBMC geodetic network were used to compute regional maps of the vertical TEC. These stations are shown in Figure 9. The spatial distribution of vertical TEC was derived using the TECANALYS™ software in multiple reference station mode employing a grid approach [e.g. *Skone*, 2000]. The two-dimensional TEC maps are defined in geomagnetic latitude and local time. A further conversion to magnetic coordinates allowed extraction of TEC gradients in the north-south (magnetic) direction over Brazil.

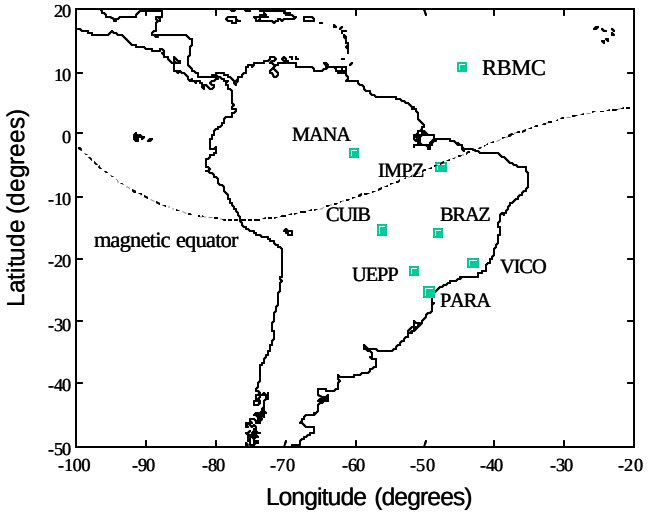

Figure 9. Permanent reference stations in the RBMC geodetic network. The magnetic equator is plotted for reference.

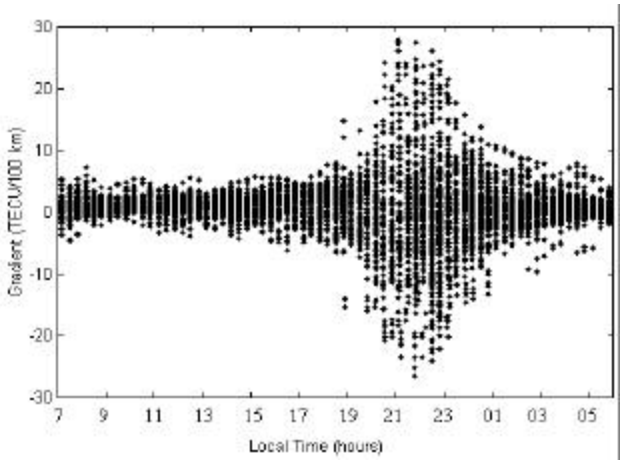

Figure 10. North-south vertical TEC gradients near the equatorial anomaly during March 2000.

Figure 10 shows the TEC gradients computed for March 2000, a period during which enhanced values of TEC were observed at low latitude station AREQ (Figure 6). Enhancement of the secondary anomaly peak is observed in the local time sector 2000-2400, where gradients as large as 20-30 TECU per 100 km (32-48 ppm for L1 ionospheric range delay) exist.

5.1.2 DGPS Position Accuracies

In order to investigate the impact of low latitude gradients on differential positioning accuracies, data from two reference stations, PARA and UEPP (Figure 9), in the Brazilian RBMC geodetic network were processed for the period 1998 – May 2000. The 430 km baseline between UEPP and PARA is aligned approximately north-south in the magnetic reference frame, and is located 15-20 degrees south of the magnetic equator – directly under the southern anomaly peak (Figure 3). DGPS accuracies are significantly degraded in this region.

As in Section 4, position estimates were derived for sample intervals of 30 s and 95th-percentile statistics were computed for every 30-minute interval. Only those estimates with HDOP (VDOP) less than 2 were included in statistics for the horizontal (vertical) DGPS position estimates. Figure 11 shows a comparison of DGPS position accuracies at reference station UEPP for each day of March 2000 and June 1999. In June, overall TEC values are lower and large gradients do not exist - such that DGPS horizontal and vertical positioning errors are on the order of 1-10 m (95th-percentile). In contrast, positioning errors of 10-50 m (95th-percentile) are observed in both vertical and horizontal components for the local time sector 2000-2400 during March 2000. Such a significant degradation in positioning accuracies can be attributed directly to the enhanced gradients observed in Figure 10.

Seasonal variations in the DGPS vertical position errors are observed in Figure 12, where the 30-minute positioning accuracies are plotted for each day of year 1999, local time sector 2000-2400. While a 24-day data gap exists during July 1999, the seasonal variations are still evident with consistently larger position errors during the winter months. An overall increase in vertical position error is also observed for late 1999 versus early 1999 – evidence of dependence on the solar cycle.

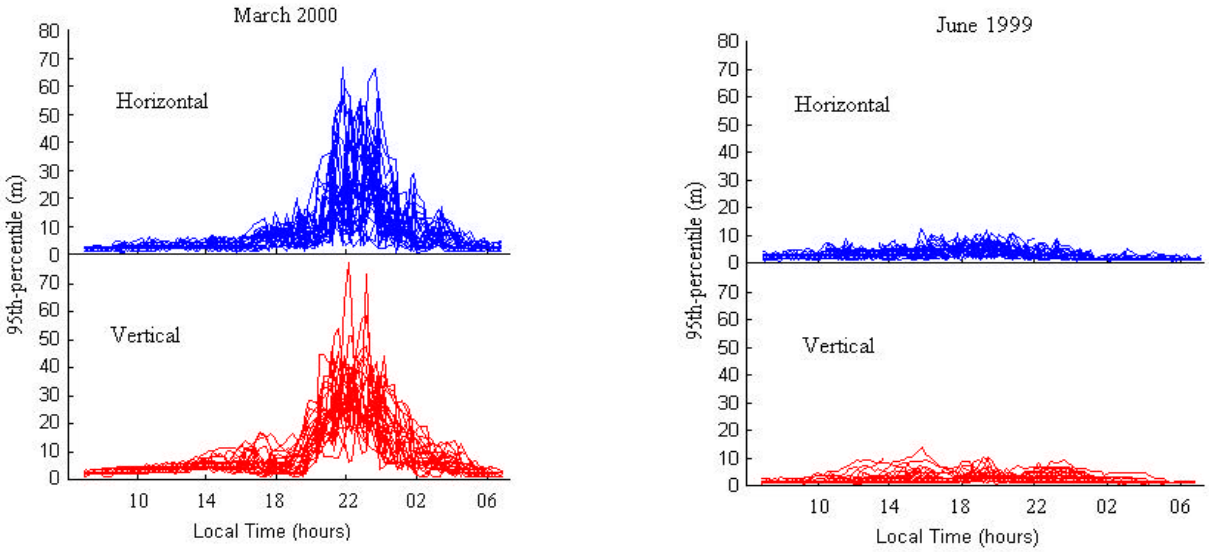

Figure 11. UEPP-PARA DGPS horizontal and vertical positioning accuracies (95th-percentile) during March 2000 and June 1999.

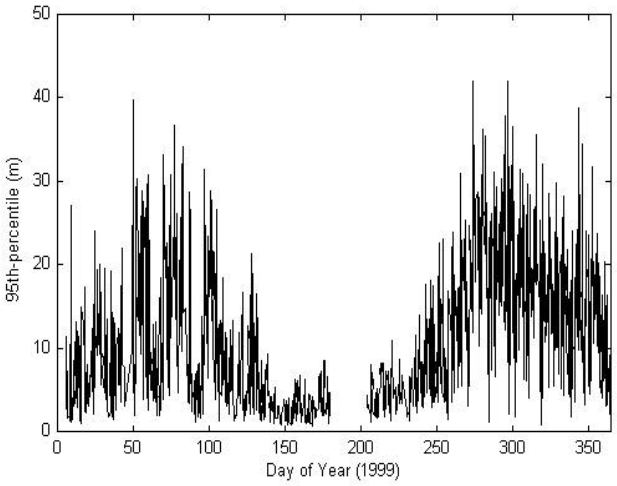

Figure 12. Seasonal variations in the UEPP-PARA DGPS vertical positioning accuracies (95th-percentile) for the local times 2000-2400.

5.2 High Latitudes

As stated in Section 2.2, the high latitude ionosphere is characterized by transient storm events. Large–scale gradients and smaller-scale irregularities in TEC are associated with these storm events and enhanced levels of ionospheric activity. The frequency of auroral substorms does not follow clear seasonal patterns and, in order to establish the impact of high latitude ionospheric phenomena on differential positioning applications, a geomagnetic index (Section 2.4) must be used to quantify the level of ionospheric activity. The magnitude of sub-auroral TEC gradients has been shown to be well-correlated with geomagnetic indices [*Vo and Foster*, 2001]. Additionally, medium-scale and small-scale irregularities in electron density are present at auroral latitudes during substorm events - such storm events are associated with the larger geomagnetic indices.

5.2.1 DGPS Position Accuracies

Marine DGPS services are offered by the Canadian Coast Guard at sub-auroral latitudes (e.g. 48°-53° geographic latitude) in the North American sector. Horizontal positioning accuracies of 10 m (95%) are specified for marine users. In order to investigate the impact of sub-auroral TEC gradients on marine DGPS positioning accuracies, position estimates were computed using two

IGS reference stations, ALBH and WILL, in Western Canada. Locations of these stations are shown in Figure 13, where the equatorward boundary of the auroral oval is plotted for a moderate storm event. These two stations are located primarily in the sub-auroral region. The 438 km baseline between ALBH and WILL is directed approximately north-south in the magnetic reference frame such that this baseline is ideal for evaluating the effects of north-south sub-auroral ionospheric gradients.

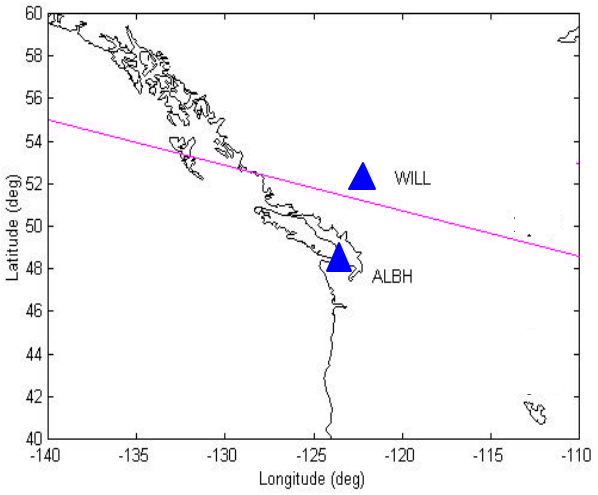

Figure 13. IGS reference stations Williams Lake (WILL) and Albert Head (ALBH) – baseline 438 km. The equatorward boundary of the auroral oval during a moderate substorm event is plotted for reference (purple line).

Observation and broadcast ephemeris files were available from both reference stations in RINEX format. Dual frequency observations were available at 30 s sample intervals. Data from three full years (1998-2000) during solar maximum were processed, and DGPS horizontal positioning errors were computed for each 30 s observation. Carrier smoothing was not applied to the observations, in order to limit the corruption of observations during periods of high ionospheric activity when carrier phase tracking may be degraded. An elevation cutoff angle of 10 degrees was applied, and an HDOP threshold of 2.0 was used.

Computed horizontal position errors were matched with the corresponding local K indices from Figure 2. These indices reflect local levels of ionospheric activity in the North American sector. Ideally, K indices from higher latitude stations closer to Western Canada should be used, as opposed to the Boulder and Fredericksburg values. No such indices were available for this analysis however.

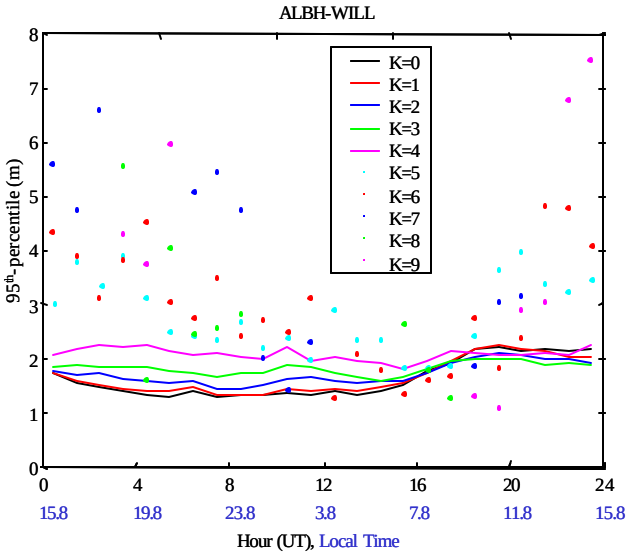

Figure 14. ALBH-WILL DGPS horizontal positioning accuracies (95th-percentile) as a function of local time and K index.

Figure 14 shows horizontal positioning accuracies versus local time for each level of ionospheric activity. In general, larger 95th-percentile values are observed for the larger K indices. Diurnal variations in positioning accuracy are also observed, reflecting the nature of ionospheric phenomena in various local time sectors. In particular, maximum positioning errors for a quiet ionosphere (K<3) are found in the dayside local time sector with a peak during the local times 1200-1400 and a minimum at local midnight. This is consistent with the diurnal variation of TEC, where larger ionospheric range errors are observed on the dayside. For enhanced levels of ionospheric activity, a similar diurnal variation is observed, with maximum positioning errors in the dayside local time sector.

The larger positioning errors for K values greater than 4, versus statistics for a quiet ionosphere (K<3), may be attributed to an increase in the background level of TEC during geomagnetically disturbed periods and an enhancement of north-south TEC gradients. These large-scale gradients are associated with the trough and SED. In general, marine DGPS users may experience degradations in positioning accuracy by a factor of 2-4 for K values of 7 or more. Such levels of ionospheric activity are associated with major-intense geomagnetic storm events, however, and are observed relatively infrequently (approximately 15 periods since 1997 – Figure 2).

5.2.2 Irregularities

As stated in Section 2.2, medium-scale irregularities in TEC are present during the larger substorm events at auroral latitudes. These features are primarily observed at latitudes above 55 degrees geographic (North American sector), but may be observed at the mid-latitudes when the oval expands southward under increasing levels of ionospheric activity.

Relative TEC series for an auroral GPS reference station (CHUR) are plotted in Figure 15 for a substorm event in August 1998. Variations in these series arise from the presence of irregularities in TEC as the satellite-receiver line-of-sight moves horizontally through the ionosphere. Corresponding ionospheric pierce points are plotted in Figure 16. The relative TEC series are calculated using Equation 4. Under average ionospheric conditions, the series plotted in Figure 15 would vary smoothly over time. The high frequency variations observed in Figure 15 arise from the presence of TEC irregularities.

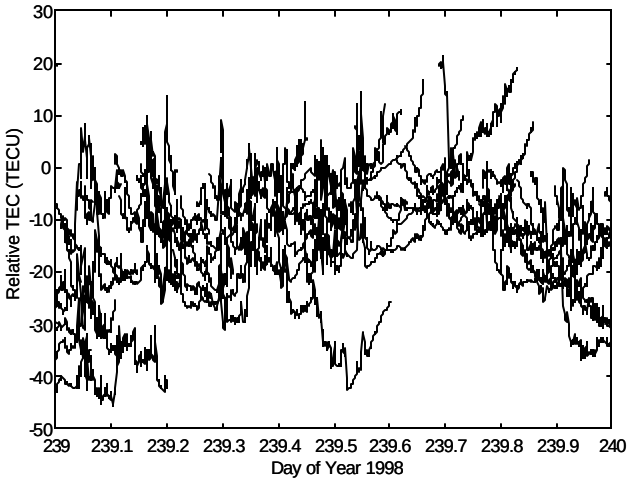

Figure 15. Relative TEC variations for each satellite observed from Churchill (CHUR) for a substorm event (K=8) August 27, 1998. Series are offset for comparison purposes.

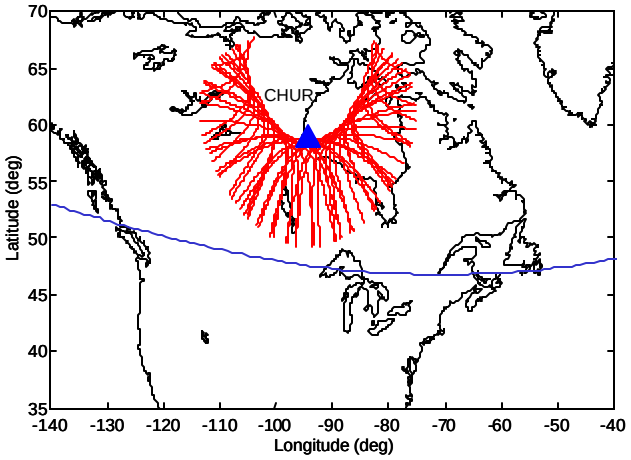

Figure 16. Line-of-sight ionospheric pierce points for reference station Churchill (CHUR) corresponding to Figure 15. The equatorward boundary of the auroral oval (moderate activity) is plotted for reference.

The rotational period of the GPS satellites is approximately 12 hours, such that the satellite-receiver line-of-sight moves through various regions of the ionosphere over time. Variations in the TEC time series therefore arise from both temporal changes in the number of ionospheric electrons, and the spatial distribution of irregularities in electron density. While it is difficult to separate spatial and temporal effects, approximate estimates of the correlation distances, wavelengths and amplitudes associated with auroral disturbances can be derived from such discrete time series through spectral analysis.

Spectral analysis of ionospheric disturbances was conducted in *Skone* [2001] for the August 1998 substorm event in the Scandinavian sector. Details of this analysis are included in the reference and only the results are quoted here. Observed fluctuations in high latitude TEC series were similar to those plotted in Figure 15. Amplitudes of 35 cm (L1) were derived for TEC features with wavelengths in the range 20-200 km. Double difference TEC values of up to 10 TECU (1.6 m L1 ionospheric range delay) were observed for a 145 km baseline.

In some cases, it is possible to reduce these ionosphere residuals by using stochastic modelling techniques [*Odijk*, 2000] and/or a regional network approach [*Liao and Gao*, 2000]. The reliability of such techniques depends on factors such as station spacing and network geometry, however, and enhanced differential range errors can limit ambiguity resolution - particularly for real-time applications.

6. GPS RECEIVER TRACKING PERFORMANCE

GPS receiver tracking performance may be degraded at high and low latitudes [*Knight et al*., 1999, *Nichols et al*., 1999]. Rapid phase variations (phase scintillations) cause a Doppler shift in the GPS signal, which may exceed the bandwidth of the phase lock loop (PLL), resulting in a loss of phase lock. Additionally, amplitude fades can cause the signal-to-noise-ratio (SNR) to drop below receiver threshold, resulting in loss of code lock. These effects have a larger impact on tracking loops employing codeless and semicodeless technologies (to extract the encrypted L2 signal) versus full code correlation. Availability of the L2 signal is particularly important for positioning applications that require formation of widelane and/or ionosphere-free observables. The magnitude and frequency of low latitude scintillations are well-correlated with seasonal enhancements of the equatorial anomaly. High latitude scintillations are generally associated with specific substorm events in the auroral zone. In this section, an overview of scintillation effects in the high, middle and low latitude regions is presented.

6.1 Data Analysis

For the purposes of this investigation, dual frequency 30 s observations were analysed from three permanent reference stations (Figure 17). Two of the stations, CENA and NLGN, form part of the CORS (Continuously Operating Reference Stations) GPS network, which includes the Continental United States and Alaska. CENA and NLGN are operated by the NGS/NOAA. The third station BRAZ is part of the RBMC geodetic network (Figure 7). Each station was equipped with a Trimble 4000 SSi (codeless) receiver such that observed variations in receiver tracking performance (between stations) may be attributed to regional ionospheric effects as opposed to differences in the receiver tracking algorithms. Observation and broadcast ephemeris files were available from each station in RINEX format, with an observation sample interval of 30 s. Data from the period 1998-2001 were analysed. By considering receiver tracking statistics from several stations in different regions over a period of years, the spatial and temporal extent of degraded tracking performance may be established.

The receiver tracking performance is quantified in terms of both the number of cycle slips detected and the number of observations missing during reacquisition periods. It is necessary to consider the number of missing observations as an additional statistic in order to accurately reflect the range of receiver performance. For receivers with long reacquisition periods, ten or twenty (or more) observations may be missing during data dropouts following loss of lock. In such cases only one cycle slip will be detected, but the impact on positioning applications is significant in terms of data dropouts. Cycle slip detection is based on the robust algorithm developed by *Blewitt* [1990]. Only those observations at elevation angles greater than 15 degrees were considered in order to eliminate tracking errors due to multipath and lower SNR.

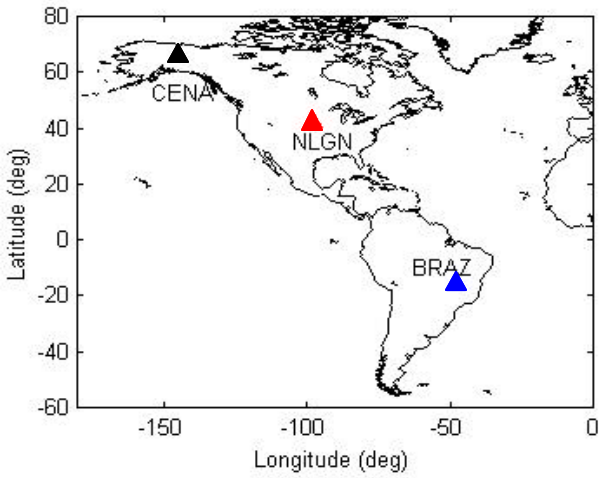

Figure 17. CORS reference stations CENA and NLGN, and RBMC reference station BRAZ. All three stations are equipped with Trimble 4000 SSi receivers.

6.2 L1 and L2 Phase Tracking Performance

An evaluation of receiver tracking performance at the three stations was performed, where L2 tracking performance was quantified in terms of the hourly percentage of L2 phase cycle slips and missing observations. These hourly percentages are plotted in Figure 18 for the entire period 1998-2001. Note that no data were available for NLGN until mid-1999. The larger percentages of corrupt observations are derived for the low latitude station BRAZ, where a clear seasonal dependence exists. The largest low latitude percentages are found in the winter months, consistent with an enhancement of the equatorial anomaly observed in Section 3. Statistics in the range 20-40 percent are observed relatively regularly at the high latitude station CENA – these values are associated with substorm activity in the auroral region. Such activity does not exhibit a strong dependence on season or solar cycle. The number of corrupt observations is generally much lower at mid-latitude station NLGN, on the order of 1-2 percent. Tracking statistics exceed 20 percent at NLGN only during limited periods when intense auroral activity has

expanded equatorward over the middle latitudes. Such intense events (K>7) are observed only rarely (Figure 2).

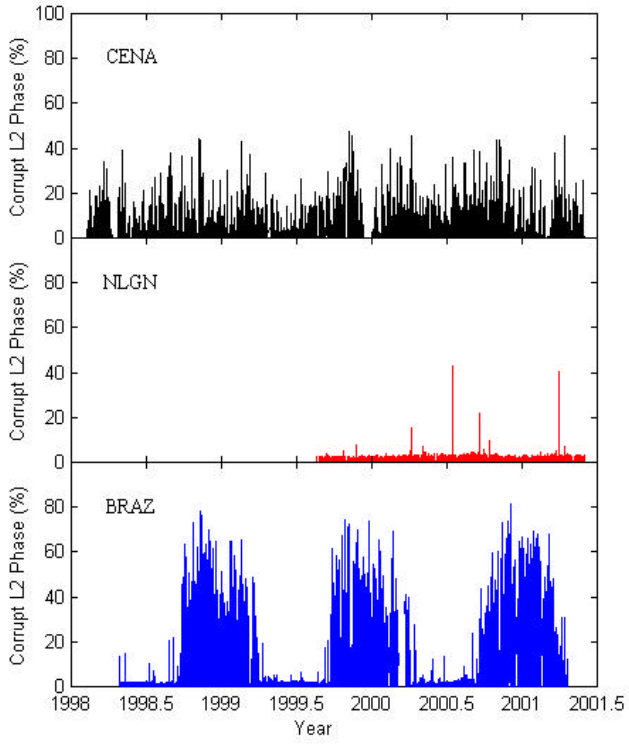

Figure 18. Hourly percentage of corrupt L2 phase observations at high (CENA), middle (USNO) and low (BRAZ) latitude GPS reference stations.

The number of one-hour periods during which receiver tracking errors exceeded 5 percent are plotted in Figure 19 as a function of local time, for the high and low latitude stations. Degraded receiver tracking performance is observed most frequently during the nighttime hours at CENA. This results from the nature of high latitude ionospheric phenomena, where the physical processes creating the aurora take place primarily in the nightside local time sector. Low latitude scintillations (BRAZ) are strongest for the local times 2000-2400 – consistent with the secondary diurnal peak of the equatorial anomaly. Tracking errors at BRAZ exceeded 60 percent most frequently at 2100 local time. For both the high and low latitude stations, minimal scintillation effects are observed in the dayside sector.

An analysis of L1 phase tracking performance was also conducted for the three reference stations. Hourly percentages of corrupt L1 phase observations were computed in the same manner as the L2 phase tracking statistics. The L1 statistics were consistently on the order of 1-2 percent for the middle and high latitude stations, even during major substorm events. Significant seasonal variations in receiver tracking performance were observed at low latitude station BRAZ, however, as shown in Figure 20. Prior to mid-1999, 20-40 percent corrupt L1 observations were observed frequently during the winter months. After a firmware upgrade in mid-1999, however, the number of corrupt L1 phase observations rarely exceeded 10 percent.

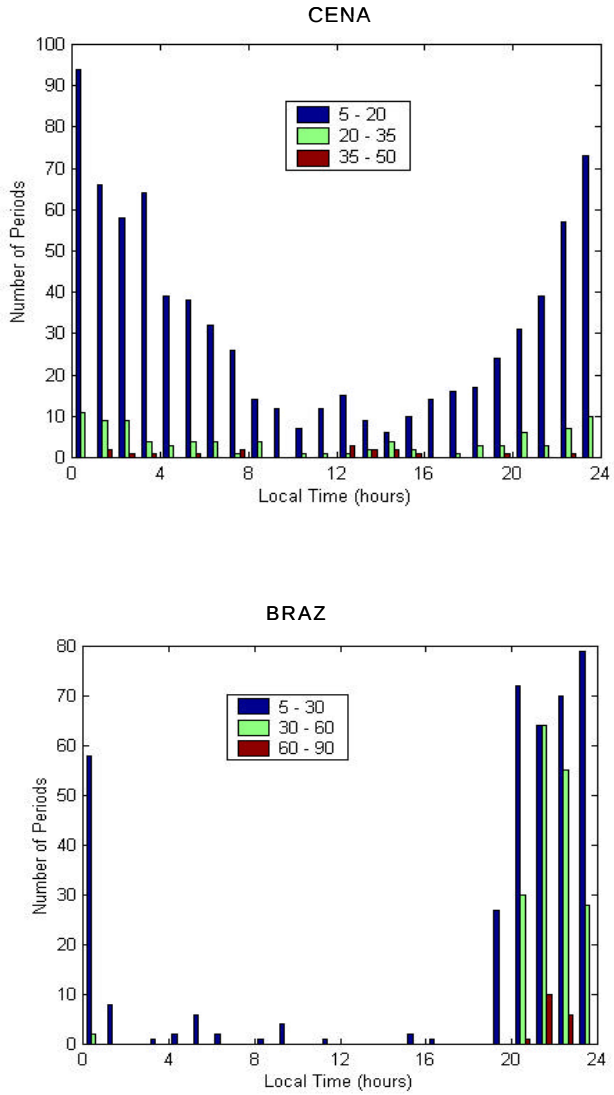

Figure 19. Number of periods for each hour of local time during which hourly percentages of corrupt L2 phase observations were in the range 5-20%, 20-35% and 35-50% at CENA; and in the range 5-30%, 30-60% and 60-90% at BRAZ.

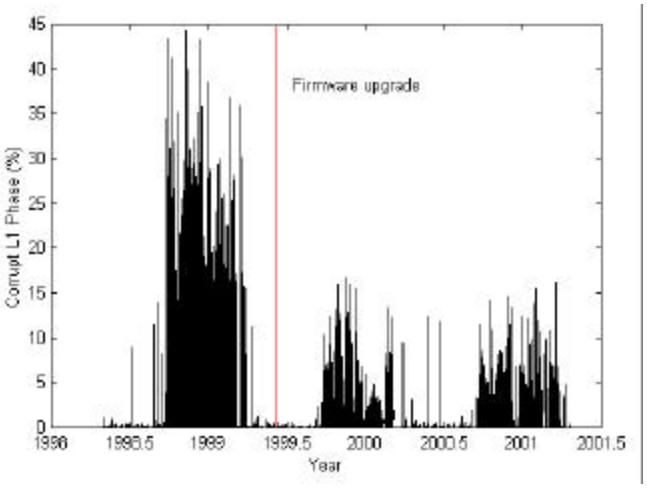

Figure 20. Hourly percentage of corrupt L1 phase observations at low latitude GPS reference station BRAZ.

It is important to note that receiver tracking performance may vary widely for different manufacturers, tracking technologies, and firmware versions (e.g. Figure 20). *Skone and Knudsen* [2001] conducted a receiver performance comparison for codeless (Trimble 400 SSi) and semicodeless (NovAtel MiLLennium and Ashtech Z-12) receivers. It was observed that L2 cycle slips were followed by long reacquisition periods for the codeless receiver, resulting in a significant number of missing observations. These long periods of missing data were not observed for the semicodeless receivers. The statistics presented in this section were derived for the Trimble 4000 SSi (codeless) receiver. It is possible that results may be significantly improved for semicodeless receivers, although the general trends (seasonal and diurnal variations) should be similar.

7. CONCLUSIONS

The impact of ionospheric phenomena on GPS positioning accuracies and receiver tracking performance has been investigated during a period of solar maximum (1998-2001). The peak of the current solar cycle occurred mid-2000, and an enhancement in the magnitude of global TEC was observed at the solar cycle peak. Additionally, seasonal variations in TEC were observed at all latitudes, with larger annual values during the equinoctial months. Regional variations in TEC also exist, with dayside TEC values being a factor of 2 larger at the low latitudes, versus the middle and high latitudes.

Degradations in vertical single point positioning accuracies were observed to be well-correlated with the absolute magnitude of TEC, with dayside positioning errors in the range 2-60 m (95%) depending on geographic location and season. Vertical single point positioning accuracies may be adequate for various single frequency applications at the higher latitudes, but error bounds differ significantly in the equatorial region.

DGPS positioning accuracies are degraded for both the vertical and horizontal components at low latitudes, in the local time sector 2000-2400. Errors arise from the presence of large-scale gradients in TEC near the secondary peak of the equatorial anomaly. This feature is enhanced during the winter months and a spatial decorrelation of approximately 40 ppm has been observed. DGPS positioning accuracies of 10-50 m (95%) were observed in the evening local time sector.

DGPS horizontal positioning accuracies were also investigated in the sub-auroral region, where large-scale gradients in TEC can exist during periods of enhanced ionospheric activity. Such gradients are not strongly dependent on season or sunspot number, although larger gradients do tend to be observed during periods of solar maximum. It was determined that DGPS horizontal positioning accuracies may be degraded by a factor of 2-4 for the higher levels of ionospheric activity. This is an issue for marine DGPS users who require metre-level accuracy for surveying applications.

Medium-scale irregularities in TEC exist at auroral latitudes during substorm events. Such features have wavelengths in the range 20-200 km and amplitudes of 35 cm (L1). While these irregularities have minimal impact on single point positioning accuracies, precise differential positioning applications may be affected and ambiguity resolution limited. It is important to consider the temporal and spatial properties of these disturbances when designing regional networks for RTK applications.

Degradations in receiver tracking performance for the L2 signal were observed in both the high and low latitude regions. The high latitude tracking performance was degraded during auroral substorm events in the nightside local time sector. Such events have occurred relatively frequently during the period 1998-2001. For the more intense events, 20-40% of L2 phase observations were corrupt. Larger percentages of tracking errors were observed at the low latitudes, where scintillation effects were found to have a strong seasonal dependence. Percentages as large as 60-80% were commonly observed in the local time sector 2000-2400 during the winter months. High percentages of corrupt L2 phase observations were observed only rarely at the mid-latitudes during severe storm events. Significant degradations in L1 phase tracking performance were observed only for the low latitudes, with 5-10% corrupt observations during the winter months.

ACKNOWLEDGEMENTS

The authors acknowledge the CORS network (NGS/NOAA), the IGS network and the IBGE, Department of Geodesy, for providing GPS data.

REFERENCES

Aarons, J., J.A. Klobuchar, H.E. Whitney, J. Austen, A.L. Johnson and C.L. Rino, Gigahertz scintillations associated with equatorial patches, *Radio Science*, 18, no. 3, 421, 1983.

Appleton, E.V., The anomalous equatorial belt in the F2-layer, *Journal of Atmopheric and Terrestrial Phys*ics, 5, 349, 1954.

Basu, S., E. Mackenzie, S. Basu, HC. Carlson, D.A. Hardy and F.J. Rich, Coordinated measurements of low-energy electron precipitation and scintillations/TEC in the auroral oval, *Radio Science*, 18, no. 6, 1151, 1983.

Basu, S, E. Mackenzie and S. Basu, Ionospheric constraints on VHZF/UHF ommunication links during solar maximum and minimum periods, *Radio Science*, 23, 363, 1988.

Blewitt, G., An automatic editing algorithm for GPS data, *Geophysical Research Letters*, 17, no. 3, 199, 1990.

Foster, J.C., Quantitative investigation of ionospheric density gradients at mid latitudes, *Proceedings of the ION National Technical Meeting*, Anaheim, California, 2000.

Huang, Y.-N. and K. Cheng, Ionospheric disturbances at the equatorial anomaly crest region during the March 1989 magnetic storm, *Journal of Geophysical Research*, 96, no. A8, 13953, 1991.

Hunsucker R.D., C. Coker, J. Cook, G. Lott, An investigation of the feasibility of utilizing GPS/TEC "signatures" for near-real time forecasting of auroral-E propagation at high-HF and low-VHF frequencies, *IEEE Transactions on Antennas and Propagation*, 43, 10, 1313, 1995.

Klobuchar, J.A., P.H. Doherty and B. El-Arini, Potential ionospheric limitations to GPS wide-area augmentation system, *NAVIGATION: Journal of the Institute of Navigation*, 42, 353, 1995.

Knight, M., M. Cervera and A. Finn, A comparison of predicted and measured GPS performance in an ionospheric scintillation environment, *Proceedings of the ION GPS-99*, Nashville, Tennessee, September, 1999.

Kunches, J.M., Now it gets interesting: GPS and the onset of solar cycle 23, *Proceedings of the ION GPS-97*, Kansas City, Missouri, 1997.

Liao, X. and Y. Gao, Carrier-based ionosphere recovery using a regional area GPS network: preliminary results. *Proceedings of the ION National Technical Meeting*, Anaheim, California, 2000.

Mayaud, P.N., *Derivation, Meaning, and Use of Geomagnetic Indices*, AGU, Washington, D.C., 1980.

Nichols, J., A. Hansen, T. Walter and P. Enge, High latitude measurements of ionospheric scintillation using the NSTB, *Proceeedings of the ION National Technical Meeting*, San Diego, California, January, 1999.

Odijk, D., Weighting ionospheric corrections to improve fast GPS positioning over medium distances, *Proceedings of the ION GPS-2000*, Salt Lake City, Utah, 2000.

Parkinson, B.W. and P.K. Enge, Differential GPS. In: Parkinson BW, Spilker JJ (ed) *Global Positioning System: Theory and Applications*, Vol. II, American Institute of Aeronautics and Astronautics, Washington, D.C, 1996.

Shaw, M., K. Sandhoo and D. Turner, Modernization of the Global Positioning System, *GPS World*, September, 2000.

Skone, S., Wide area ionosphere modeling in the equatorial region during a magnetic storm event. *Proceedings of the ION National Technical Meeting*, Anaheim, California, 2000.

Skone S. and K. Knudsen, GPS receiver tracking performance under equatorial and high latitude ionospheric scintillations, 3rd International Symposium on Mobile Mapping Technology, Cairo, Egypt, 2001.

Skone, S.H., The Impact of Magnetic Storms on GPS Receiver Performance, *Journal of Geodesy*, 2001 (in press).

Soicher, H. and F.J. Gorman, Seasonal and day-to-day variability of total electron content at mid-latitudes near solar maximum, *Radio Science*, 20, no. 3, 383, May-June, 1985.

Vo, H. and J.C. Foster, A quantitative study of ionospheric density gradients at mid-latitudes, *Geophysical Research Letters*, 2001 (in press).

Wanninger, L., Effects of equatorial ionosphere on GPS, *GPS World*, July, 1993.